Johann Radon Institute for
Computational and Applied Mathematics
Austrian Academy of Sciences (ÖAW)

Conditional space-time stability of collocation Runge–Kutta for parabolic evolution equations

R. Andreev, J. Schweitzer

RICAM-Report 2013-15

CONDITIONAL SPACE-TIME STABILITY OF COLLOCATION RUNGE–KUTTA FOR PARABOLIC EVOLUTION EQUATIONS

ROMAN ANDREEV AND JULIA SCHWEITZER

Abstract. We formulate collocation Runge–Kutta time-stepping schemes applied to linear parabolic evolution equations as space-time Petrov–Galerkin discretizations, and investigate their a priori stability for the parabolic space-time norms, that is the continuity constant of the discrete solution mapping. We focus on collocation based on A-stable Gauss–Legendre and L-stable right-Radau nodes, addressing in particular the implicit midpoint rule and the backward Euler time-stepping schemes. Collocation on Lobatto nodes is analysed as a by-product. We find through explicit estimates that the continuity constant is controlled in terms of the parabolic CFL number together with a measure of self-duality of the spatial discretization. Numerical observations motivate and illustrate the results.

1. Introduction

1.1. **Introduction and model problem.** The aim of this paper is to identify conditions on the discretization parameters under which collocation Runge–Kutta time-stepping schemes for linear parabolic evolution equations are a priori stable as space-time Petrov–Galerkin methods. Space-time stability is of central interest for instance for space-time simultaneous solution and preconditioning of the parabolic evolution equation, and for residual based a posteriori error estimation.

To clarify this statement, we begin by introducing the necessary notation and the linear parabolic evolution equation that we are going to study.

Let V be a real separable Hilbert space continuously and densely embedded in another, $V \hookrightarrow H$. The Hilbert space H is identified with its dual via the Riesz isomorphism. An example will be provided by Sobolev spaces or closed subspaces thereof. By V' we will denote the dual of V that collects all bounded linear functionals on V. We write $\|\cdot\|_V$ for the norm of V, etc. The scalar product on H, as well as the duality pairing between V and V' will be denoted by $(\cdot,\cdot)$. Let $A : V \to V'$ be a bounded linear operator satisfying the coercivity condition

$$(A\chi,\chi) \geq \alpha^2\|\chi\|_V^2 - \gamma^2\|\chi\|_H^2 \quad \forall \chi \in V \tag{1}$$

for some fixed $\alpha > 0$ and $\gamma \geq 0$. Let $J = (0,T)$ be a nonempty bounded interval. Consider the Bochner spaces

$$X = H^1(J;V') \cap L^2(J;V) \quad \text{and} \quad Y := H \times L^2(J;V)$$

equipped with the norms given by

$$\|w\|_X^2 := \|\partial_t w\|_{L^2(J;V')}^2 + \|w\|_{L^2(J;V)}^2 + \|w(T)\|_H^2, \quad w \in X, \tag{2}$$

$$\|v\|_Y^2 := \|v_0\|_H^2 + \|v_1\|_{L^2(J;V)}^2, \quad v = (v_0,v_1) \in Y. \tag{3}$$

Date: October 7, 2013.

2010 *Mathematics Subject Classification.* 35K90, 65M12, 65M20, 65M60.

Omitting the last term $w(T)$ of $\|\cdot\|_X$ yields and equivalent norm, albeit not uniformly in the length of J, by continuity of the embedding $X \hookrightarrow C^0(\bar{J};H)$, see [9, Chapter 1]. The present choice, however, simplifies some estimates such as the result of Lemma 3.2. In the following we identify Y' with $H \times L^2(J;V')$, and where convenient also $L^2(J;V) \cong L^2(J) \otimes V$, and $H^1(J;V) \cong H^1(J) \otimes V$ isometrically, similarly for other Hilbert spaces. The symbol $\otimes$ denotes the tensor product of Hilbert spaces or of linear operators.

Fundamental to the present paper is the fact: *The linear parabolic evolution equation*

$$(\partial_t + A)u(t) = f(t) \in V' \quad \textit{(a.e.) } t \in J, \qquad u(0) = g \in H, \tag{4}$$

defines an isomorphism between X and Y'. In other words, the mapping $X \to Y'$, $u \mapsto (g,f)$, is bounded and linear, with a bounded inverse. This is in fact true even if A is allowed to depend (weak-star) measurably on t with uniform continuity and coercivity bounds, see for instance [9, Chapter 3, Section 4.7], but for our purposes it will suffice to assume that A is constant in the time variable t. We moreover assume that A is self-adjoint and that $\gamma = 0$ in (1), that is

$$(A\chi, \widetilde{\chi}) = (\chi, A\widetilde{\chi}) \quad \text{and} \quad (A\chi,\chi) \geq \alpha^2 \|\chi\|_V^2 \quad \forall \chi, \widetilde{\chi} \in V. \tag{5}$$

Given a source term $f \in L^2(J;V')$ and an initial datum $g \in H$, the parabolic evolution equation can be equivalently formulated as the linear operator equation

$$\text{find} \quad u \in X \quad \text{s.t.} \quad B(u,v) = F(v) \quad \forall v \in Y, \tag{6}$$

where the bilinear form $B : X \times Y \to \mathbb{R}$ and the linear functional $F \in Y'$, given by

$$B(w,v) := \int_J ((\partial_t + A)w, v_1)dt + (w(0), v_0), \quad (w,v) \in X \times Y, \tag{7}$$

$$F(v) := \int_J (f, v_1)dt + (g, v_0), \quad v = (v_0, v_1) \in Y, \tag{8}$$

are both well-defined and bounded. Thus, the temporal evolution is enforced in (6) by testing with functions $v_1 \in L^2(J;V)$, while the initial condition is enforced by testing with $v_0 \in H$.

We occasionally omit the specification of the norm if clear from the context, for instance the norm of B is denoted by $\|B\|$. Generally, we omit the t-dependence of the integrands in the notation.

1.2. **Space-time stability.** Runge–Kutta time-stepping schemes are among the classical numerical solution methods for evolution equations such as (4). In this paper we focus on the subclass of collocation Runge–Kutta time-stepping schemes because these are, in the sense specified below, equivalent to piecewise polynomial in time Petrov–Galerkin methods for the space-time variational formulation (6). For (nonlinear) ordinary differential equations this equivalence was observed for instance in [8]. Broadly speaking, a collocation Runge–Kutta time-stepping scheme with a possible semi-discretization of V applied to the parabolic evolution equation (4) coincides with the solution to the conforming Petrov–Galerkin space-time variational formulation

$$\text{find} \quad u_h \in X_h \quad \text{s.t.} \quad B(u_h, v_h) = F(v_h) \quad \forall v_h \in Y_h \tag{9}$$

for certain closed subspaces $X_h \subset X$ and $Y_h \subset Y$ containing piecewise polynomial functions on the temporal interval J with values in (a closed subspace of) V. Herein, the subscript $h > 0$ encodes the discretization parameters such as the temporal mesh, the polynomial degrees involved, etc., and we presuppose that the span of $\bigcup_{h>0} X_h$ is dense in X. This interpretation

raises the usual question of *stability* of Petrov–Galerkin discretizations, namely whether the continuous dependence on the data of the exact solution is also true for the discrete solution: does there exist a constant $C_h > 0$ such that for any $F \in Y'$ the solution of (9) satisfies

$$\|u_h\|_X \leq C_h \|F\|_{Y'} \tag{10}$$

and how does C_h depend on the discretization parameter h? This question reduces to the study of the discrete inf-sup constant

$$\gamma_h := \inf_{w_h \in X_h \setminus \{0\}} \sup_{v_h \in Y_h \setminus \{0\}} \frac{B(w_h, v_h)}{\|w_h\|_X \|v_h\|_Y} \tag{11}$$

because the estimate $C_h \leq \gamma_h^{-1} \|B\|$ holds for the constant in (10). We shall speak of *space-time stability* if uniform stability

$$\inf_{h>0} \gamma_h > 0 \tag{12}$$

occurs.

In a special case we can estimate the operator norm of the bilinear form B. First, $|B(w,v)|$ is at most $\|v\|_Y$ times the square root of $\|(\partial_t + A)w\|^2_{L^2(J;V')} + \|w(0)\|^2_H$ for all $w \in X$ and all $v \in Y$. Assume now that the linear operator A in addition to being positive and self-adjoint, is an isometry. Expanding the norm of $(\partial_t + A)w$ and evaluating $2\int_J (\partial_t w, Aw) dt = \|w(T)\|^2_H - \|w(0)\|^2_H$ we arrive at $|B(w,v)| \leq \|w\|_X \|v\|_Y$. Hence, $\|B\| \leq 1$.

As alluded to at the beginning of this section, our aim is to identify conditions on the discretization parameters under which collocation Runge–Kutta time-stepping schemes for the linear parabolic evolution equation (4) are space-time stable in the sense of (12). Thus we are interested in an a priori analysis, and in contrast to the typical convergence analysis for Runge–Kutta time-stepping schemes, we do not assume any additional temporal smoothness of the exact solution or the residual, or regularity of the initial datum. The a priori convergence analysis usually proceeds via the quasi-optimality estimate

$$\|u - u_h\|_X \leq \frac{\|B\|}{\gamma_h} \inf_{w_h \in X_h} \|u - w_h\|_X,$$

which is valid for conforming Petrov–Galerkin discretizations [11], and highlights the importance of the discrete inf-sup constant (11).

For collocation Runge–Kutta time-stepping based on Gauß–Legendre nodes, our findings are in essence similar to the those of Babuška and Janik in [5], although based on a slightly different space-time variational formulation. Assumptions of [5, Theorem 3.4.1] on the relative size of the temporal elements and on the distribution of the polynomial degrees are unnecessary here, probably due to our formulating the results in terms of the local CFL number instead of the number of temporal elements. Moreover, we do not rely on the eigenbasis representation of the operator and give explicit constants. We find an additional bound which is active for large CFL numbers and is independent of the details of the temporal discretization. When this uniform bound is not active, the space-time stability constant in (10) is essentially proportional to the CFL number.

The second contribution of this work is a similar analysis for collocation Runge–Kutta time-stepping based on right-Radau nodes, whose most notable representative is the backward Euler time-stepping scheme, as well as Lobatto nodes. We find for instance that for right-Radau nodes the space-time stability constant in (10) is in general proportional to the square root of the CFL number, except in certain important situations where it is indeed of order

one. Moreover, our estimates and numerical examples indicate that Lobatto nodes is the least space-time stable choice among the three.

We remark that it may be possible, via the identification of discontinuous Galerkin and right-Radau collocation Runge–Kutta time-stepping schemes [1], to relate our results to [10]. There, space-time stability in mesh-dependent norms of a space-time discontinuous Galerkin discretization of the heat equation was obtained, interestingly, assuming that the CFL number is not too small.

In Section 2 we describe collocation Runge–Kutta time-stepping schemes, and recall their classical A- and L-stability properties. We introduce the adjoint of the polynomial interpolation operator.

In Section 3 the adjoint of the polynomial interpolation operator is used to formulate collocation Runge–Kutta time-stepping schemes equivalently as a conforming space-time Petrov–Galerkin method for the space-time variational formulation (9), which is satisfied by the exact solution to the parabolic evolution equation (4). Subsequently, we mainly focus on Gauß–Legendre and right-Radau collocation, and obtain results on Lobatto collocation as a by-product. We estimate the discrete inf-sup constant (11) in terms of the discretization parameters such as the time step size and the polynomial degrees, together with a measure of self-duality of the discretization of V. Here the parabolic CFL number appears naturally in the estimates.

We conclude in Section 4.

1.3. **Illustration.** We illustrate the kind of behavior of the stability constant C_h that we wish to exhibit and explain in this paper, exemplarily for the implicit midpoint rule and the backward Euler time-stepping schemes. These are examples of A-stable and L-stable collocation Runge–Kutta time-stepping schemes, respectively, see Section 2. On the temporal nodes the implicit midpoint rule solution coincides with that produced by the Crank–Nicolson time-stepping scheme or implicit trapezoidal rule in the present case of a linear evolution equation. We consider the heat equation as a model parabolic evolution equation (4). More precisely, the operator A is taken as the minus Laplacian on a bounded spatial domain in Euclidean space with homogeneous Dirichlet boundary conditions. The spatial domain and the spatial semi-discretization by finite elements are fixed to be those from [2, Sections 2–8], the details are immaterial for us and can be found there. The computations were done using the methods of [3], the main difference being in the choice of the norm on X. We set $T = 20$ for the end time. For both time-stepping schemes we perform N equidistant time steps. The results are summarized in Figure 1.3.

We observe, and prove in Section 3 below, the following. The space-time stability constant C_h decreases with the number of time steps N, and, when N is large enough, approaches *one* (implicit midpoint rule) and *two* (backward Euler), respectively. This happens when the parabolic CFL number (that can be thought of as time step size divided by the square of spatial mesh width, see (33) for the definition) is of order one. On the other hand, when the number of time steps is small, and the CFL number is comparatively large, the implicit midpoint rule and the backward Euler time-stepping schemes exhibit qualitatively different behavior: in the first case, C_h stagnates, and then decays proportionally to the CFL number; in the second case, C_h decays proportionally to the square root of the CFL number from the onset on. From this perspective, backward Euler is the preferable time-stepping scheme among the two, at least on an equidistant temporal mesh. The space-time stability constant, which in this toy example barely spans one order of magnitude, can be much larger for finer

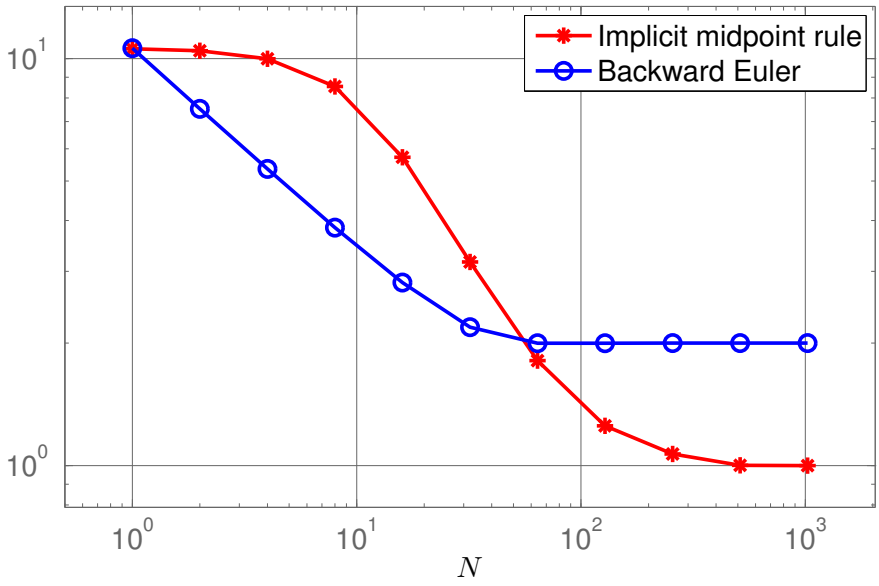

FIGURE 1. Space-time stability constant for implicit midpoint rule and backward Euler time-stepping schemes as a function of the number N of equidistant time-steps, see Section 1.3 for details.

spatial finite element discretizations containing local refinement and/or for larger temporal intervals.

Our task is to explain the behavior observed in Figure 1.3 for a certain class of collocation Runge–Kutta time-stepping schemes. These are introduced in the next section.

2. Collocation Runge–Kutta time-stepping schemes

2.1. **Construction.** A finite set of temporal nodes of the form $\mathcal{T} = \{0 = t_0 < t_1 < \ldots < t_N = T\}$ is called a temporal mesh. The intervals (t_{n-1}, t_n), $n = 1, \ldots, N$, are called temporal elements of $\mathcal{T}$. Given $\mathcal{T}$ with N temporal elements, for any vector of polynomial degrees $\mathbf{p} = (p_n)_{n=1}^N \in \mathbb{N}_0^N$ let $S^{0,\mathbf{p}}(\mathcal{T})$ denote the space of left-continuous functions $s : [0, T] \to \mathbb{R}$ for which $s|_{(t_{n-1},t_n]}$ is a polynomial of degree at most p_n for each element number $n = 1, \ldots, N$. We further define the space of continuous piecewise polynomials $S^{1,\mathbf{p}}(\mathcal{T}) := C^0([0, T]) \cap S^{0,\mathbf{p}}(\mathcal{T})$.

Let $V_h \subset V$ be a finite-dimensional subspace, $\mathcal{T}$ a temporal mesh, and $\mathbf{p} \in \mathbb{N}_0^N$ a vector of polynomial degrees. Recall that $V \hookrightarrow H$ and that $(\cdot, \cdot)$ denotes the scalar product in H. A collocation Runge–Kutta time-stepping scheme for the parabolic evolution equation (4) can now be described as the process of constructing $u_h : [0, T] \to V_h$ as follows: 1) Fix $u_h(0)$ requiring $(u_h(0), \chi_h) = (g, \chi_h)$ for all $\chi_h \in V_h$. 2) For each $n = 1, \ldots, N$, pick a set of p_n distinct collocation nodes $\mathcal{N}_n \subset [t_{n-1}, t_n]$, and require that the V_h-valued polynomial $u_h|_{[t_{n-1},t_n]}$ of degree p_n, of which the value $u_h(t_{n-1})$ is already known, satisfies the p_n collocation conditions

$$((\partial_t + A)u_h(\tau) - f(\tau), \chi_h) = 0 \quad \forall \tau \in \mathcal{N}_n \quad \forall \chi_h \in V_h. \tag{13}$$

If a node of $\mathcal{T}$ was chosen for collocation then the temporal derivative is understood as the one-sided derivative from within the current temporal element (t_{n-1}, t_n).

By construction, u_h is in the space $X_h := S^{1,\mathbf{p}}(\mathcal{T}) \otimes V_h$ of continuous V_h-valued piecewise polynomial functions on $[0,T]$. As in [1, Equation (2.17)], we can replace the collocation conditions (13) by

$$(\partial_t u_h + I_{\mathcal{N}_n}(Au_h - f), \chi_h) = 0 \quad \text{on} \quad [t_{n-1}, t_n] \quad \forall \chi_h \in V_h,$$

where $I_{\mathcal{N}_n}$ denotes the polynomial interpolation operator on the collocation nodes $\mathcal{N}_n$ by a polynomial of degree $(p_n - 1)$. Let $I_{\mathcal{N}}$ denote the compound interpolation operator that produces a piecewise polynomial in $S^{0,\mathbf{p}-1}(\mathcal{T})$. Set $Y_h := V_h \times [S^{0,\mathbf{p}-1}(\mathcal{T}) \otimes V_h]$. Then the whole process can be formulated as:

$$\text{find} \quad u_h \in X_h \quad \text{s.t.} \quad B_{\mathcal{N}}(u_h, v_h) = F_{\mathcal{N}}(v_h) \quad \forall v_h \in Y_h, \tag{14}$$

where $B_{\mathcal{N}}$ is defined as in (7) with Au replaced by $I_{\mathcal{N}}Au$, and $F_{\mathcal{N}}$ is defined as in (8) with f replaced by $I_{\mathcal{N}}f$.

The latter space-time variational formulation (14) suffers from the drawback that the source $f \in L^2(J; V')$ needs to have some more regularity for $I_{\mathcal{N}}f$ to be well-defined. We shall instead show that there are subspaces Y_h for which the same u_h is obtained from the discrete variational formulation (9) with the original definitions of the bilinear form B and the functional F whenever f is a piecewise polynomial in $S^{0,\mathbf{p}}(\mathcal{T}) \otimes V'$.

Before doing so, let us recall the classical notions of stability, here only for collocation Runge–Kutta time-stepping schemes of the above type.

2.2. **Classical stability properties.** For any set of distinct collocation nodes $\mathcal{N} \subset \mathbb{R}$ let $\Pi_{\mathcal{N}}$ denote the polynomial $\Pi_{\mathcal{N}} : t \mapsto \prod_{\tau \in \mathcal{N}}(t - \tau)$, with the convention $\Pi_\emptyset := 1$. Let $\mathcal{N} \subset [0,1]$ be a set of distinct collocation nodes, and $z \in \mathbb{C}$. Define the polynomial $y : \mathbb{R} \to \mathbb{C}$ of degree $\#\mathcal{N}$ by $y(0) = 1$ and the collocation conditions $y'(\tau) = zy(\tau)$ for $\tau \in \mathcal{N}$. Set $R_{\mathcal{N}}(z) := y(1)$, which is called the stability function of $\mathcal{N}$. Then $\mathcal{N}$ is called A-stable if $|R_{\mathcal{N}}(z)| \le 1$ for all $z \in \mathbb{C}$ with $\operatorname{Re} z \le 0$, and it is called L-stable if in addition $R_{\mathcal{N}}(-\infty) := \lim_{z\to\infty} R_{\mathcal{N}}(-z) = 0$. We do not consider more refined notions of stability of time-stepping schemes, see for instance [7, Section V.9]. By [7, Theorem 3.10], the stability function is the rational function $R_{\mathcal{N}}(z) = Q_1(z)/Q_0(z)$ with $Q_t(z) := \sum_{j\ge 0} \Pi_{\mathcal{N}}^{(j)}(t) z^{-j}$. This representation implies that $\mathcal{N}$ can only be L-stable if $1 \in \mathcal{N}$.

Let $\mathbb{P}_d$ denote the space of polynomials of degree at most d. If $d < 0$ then $\mathbb{P}_d := \{0\}$. For each $d \in \mathbb{N}$, let $\mathcal{G}_d \subset (0,1)$, $\mathcal{R}_d \subset (0,1]$, and $\mathcal{L}_d \subset [0,1]$ denote the d Gauß–Legendre, the right-Radau, and the Lobatto nodes for the interval $[0,1]$, respectively. These are characterized [6, Theorem 1.4.5] by requiring $1 \in \mathcal{R}_{d+1}$ and $\{0,1\} \subset \mathcal{L}_{d+2}$ for all $d \ge 0$, and $\int_0^1 \Pi_{\mathcal{N}}(t)p(t)dt = 0$ for all $p \in \mathbb{P}_{d-1}$, $\mathcal{N} \in \{\mathcal{G}_d, \mathcal{R}_{d+1}, \mathcal{L}_{d+2}\}$, $d \ge 1$. The implicit midpoint rule is the collocation Runge–Kutta time-stepping scheme based on $\mathcal{G}_1$, while backward Euler with piecewise linear reconstruction corresponds to $\mathcal{R}_1$.

The unique rational polynomial of numerator degree k and denominator degree j that approximates the exact solution $y : z \mapsto e^z$ up to an error of $\mathcal{O}(z^{j+k+1})$, as $z \to 0$, is called (k,j)-Padé approximation [7, Theorem 3.11]. It follows that $R_{\mathcal{G}_d} = R_{\mathcal{L}_{d+1}}$ is the (d,d)-Padé approximation and $R_{\mathcal{R}_d}$ is the $(d-1,d)$-Padé approximation, and each is A-stable [7, Theorem 4.12]. However, only the right-Radau nodes are L-stable, $R_{\mathcal{R}_d}(-\infty) = 0$, because the denominator has higher polynomial degree than the numerator. This is the fundamental difference between the implicit midpoint rule and the backward Euler time-stepping schemes.

2.3. **The adjoint of the interpolation operator.** For any polynomial π, its span is denoted by $\mathbb{R}\pi$. Recall the notation $\Pi_{\mathcal{N}} : t \mapsto \prod_{\tau\in\mathcal{N}}(t-\tau)$ with $\Pi_\emptyset := 1$. For any set $\mathcal{N} \subset [0,1]$ of d distinct collocation nodes let $I_{\mathcal{N}}$ be the polynomial interpolation operator on $\mathcal{N}$. We define the operator $I^\star_{\mathcal{N}}$ by

$$I^\star_{\mathcal{N}} : \mathbb{P}_{d-1} \to \mathbb{P}_d, \quad q \mapsto q - \frac{(q,\Pi_{\mathcal{N}})_{L^2(0,1)}}{(L_d,\Pi_{\mathcal{N}})_{L^2(0,1)}} L_d, \tag{15}$$

where L_d is the Legendre polynomial of degree d on $[0,1]$, which is orthogonal to all polynomials of lower degree in $L^2(0,1)$. Throughout, the Legendre polynomials are normalized to unit norm in L^2. Many useful properties of orthogonal polynomials can be derived from their recurrence formulae, see [6, §1.3.2]. For instance, for future purposes we note that $L_d(1) = \sqrt{2d+1}$. Since $\Pi_{\mathcal{N}}$ has degree d, the denominator in (15) is nonzero. Obviously, the inverse of $I^\star_{\mathcal{N}}$ is given by $p \mapsto p - (p, L_d)_{L^2(0,1)} L_d$, which is a contraction on $L^2(0,1)$. The reason for the notation is the following observation.

Lemma 2.1. *The mapping $I^\star_{\mathcal{N}} : \mathbb{P}_{d-1} \to \mathbb{P}_d$ defined by* (15) *is linear and injective, and*

$$(I_{\mathcal{N}} p, q)_{L^2(0,1)} = (p, I^\star_{\mathcal{N}} q)_{L^2(0,1)} \quad \forall (p,q) \in \mathbb{P}_d \times \mathbb{P}_{d-1}. \tag{16}$$

Proof. Linearity is clear, and injectivity is due to $L_d \notin \mathbb{P}_{d-1}$. To verify (16) we check it for $p \in \mathbb{P}_{d-1}$ and $p = \Pi_{\mathcal{N}}$ separately, since $\mathbb{P}_{d-1} \oplus \mathbb{R}\Pi_{\mathcal{N}} = \mathbb{P}_d$. First, if $p \in \mathbb{P}_{d-1}$ then $I_{\mathcal{N}} p = p$, and $q - I^\star_{\mathcal{N}} q \propto L_d$ is indeed orthogonal to p. Second, if $p = \Pi_{\mathcal{N}}$ then $I_{\mathcal{N}} p = 0$, but also $(\Pi_{\mathcal{N}}, I^\star_{\mathcal{N}} q)$ vanishes after simplification. □

For any set $\mathcal{N} \subset [0,1]$ of d distinct collocation nodes, we define the polynomial space

$$\mathbb{Q}_{\mathcal{N}} := I^\star_{\mathcal{N}} \mathbb{P}_{d-1} \subset \mathbb{P}_d. \tag{17}$$

Lemma 2.2. *Let $\mathcal{N} \subset [0,1]$ be a set of d distinct nodes and $p \in \mathbb{P}_d$. Then p vanishes on $\mathcal{N}$ if and only if $(p,q)_{L^2(0,1)} = 0$ for all $q \in \mathbb{Q}_{\mathcal{N}}$.*

Proof. By Lemma 2.1 and the definition (17), the operator $I^\star_{\mathcal{N}} : \mathbb{P}_{d-1} \to \mathbb{Q}_{\mathcal{N}}$ is an isomorphism. Now, the polynomial $p \in \mathbb{P}_d$ vanishes on $\mathcal{N}$ if and only if its interpolant $I_{\mathcal{N}} p$ is identically zero, that is $0 = (I_{\mathcal{N}} p, (I^\star_{\mathcal{N}})^{-1} q)_{L^2(0,1)} = (p,q)_{L^2(0,1)}$ for all $q \in \mathbb{Q}_{\mathcal{N}}$. □

We say that the nodes $\mathcal{N} \subset [0,1]$ are exact on $\mathbb{P}_d$ if the interpolatory quadrature of p on $[0,1]$ based on the nodes $\mathcal{N}$ coincides with $\int_0^1 p dt$ for all $p \in \mathbb{P}_d$. We will repeatedly use the fact [6, Section 1.4] that the Gauß–Legendre nodes $\mathcal{G}_d$ are exact on $\mathbb{P}_{2d-1}$, the right-Radau nodes $\mathcal{R}_d$ are exact on $\mathbb{P}_{2d-2}$, and the Lobatto nodes $\mathcal{L}_d$ are exact on $\mathbb{P}_{2d-3}$.

The following result characterizes the polynomial space $\mathbb{Q}_{\mathcal{N}}$ in (17) for these particular cases. We write $\mathcal{N}^\circ := \mathcal{N} \cap (0,1)$.

Proposition 2.3. *The spaces $\mathbb{Q}_{\mathcal{N}} = I^\star_{\mathcal{N}} \mathbb{P}_{d-1}$ for the Gauß–Legendre, right-Radau and Lobatto nodes are explicitly given by $\mathbb{Q}_{\mathcal{G}_d} = \mathbb{P}_{d-1}$, $\mathbb{Q}_{\mathcal{R}_d} = \mathbb{P}_{d-2} \oplus \mathbb{R}\Pi_{\mathcal{R}^\circ_{d+1}}$, and $\mathbb{Q}_{\mathcal{L}_d} = \mathbb{P}_{d-3} \oplus \mathbb{R}L_{d-1} \oplus \mathbb{R}\Pi_{\mathcal{L}^\circ_{d+2}}$.*

Proof. In each case, the spaces have the correct dimension, and all are subspaces of $\mathbb{P}_d$. By (16), we only need to check that any polynomial q from the characterizing space is orthogonal to $\Pi_{\mathcal{N}}$ for the set of nodes $\mathcal{N}$ in question. Consider $\mathcal{N} = \mathcal{L}_d$, as the other cases are similar. First, if $q \in \mathbb{P}_{d-3}$ then $(\Pi_{\mathcal{L}_d}, q)_{L^2(0,1)} = 0$ because the Lobatto nodes $\mathcal{L}_d$ are exact on $\mathbb{P}_{2d-3}$ and $\Pi_{\mathcal{L}_d} q \in \mathbb{P}_{2d-3}$ vanishes on $\mathcal{L}_d$. Second, $(\Pi_{\mathcal{N}}, L_{d-1})_{L^2(0,1)} = 0$ because the polynomials

have opposite parity around the midpoint of the interval. Finally, $(\Pi_{\mathcal{N}}, \Pi_{\mathcal{L}^\circ_{d+2}})_{L^2(0,1)} = 0$ because $\mathcal{L}_{d+2}$ are exact on $\mathbb{P}_{2d}$. □

For nodes $\mathcal{N}$ other than the Gauß–Legendre nodes, there is a "degree gap" because $\mathbb{Q}_{\mathcal{N}} \neq \mathbb{P}_{d-1}$ is d-dimensional. For instance, $\mathbb{Q}_{\mathcal{R}_1}$ is the span of $\Pi_{\{1/3\}} : t \mapsto t - 1/3$, since the $d = 2$ right-Radau nodes on the unit interval are $\mathcal{R}_2 = \{1/3, 1\}$. For the Lobatto nodes, Lemma 2.2 holds also with $\mathbb{Q}_{\mathcal{L}_d} := \mathbb{P}_{d-3} \oplus \mathbb{R}\Pi_{\mathcal{L}_{d+2}\setminus\{0\}} \oplus \mathbb{R}\Pi_{\mathcal{L}_{d+2}\setminus\{1\}}$, which is a subspace of $\mathbb{P}_{d+1}$.

The reason that the polynomial $\Pi_{\mathcal{R}^\circ_{d+1}}$ appears in Proposition 2.3 is the property

$$(\Pi, p)_{L^2(0,1)} = \frac{\|\Pi\|^2_{L^2(0,1)}}{\Pi(1)} p(1) \quad \forall p \in \mathbb{P}_d, \quad \text{where} \quad \Pi := \Pi_{\mathcal{R}^\circ_{d+1}}.$$

That is, testing a polynomial p with Π yields a multiple of the value of p at $t = 1$. Indeed, the right-Radau nodes $\mathcal{R}_{d+1}$ being exact on $\mathbb{P}_{2d}$, the left-hand-side yields a multiple of $p(1)$. The factor is determined by setting $p := \Pi$.

Since the right-Radau nodes $\mathcal{R}_d$ are exact on $\mathbb{P}_{2d-2}$, the polynomial $\Pi_{\mathcal{R}_d}$ is linear combination of the Legendre polynomials L_{d-1} and L_d. Recalling $\Pi_{\mathcal{R}_d}(1) = 0$ we find

$$\Pi_{\mathcal{R}_d} \propto L_{d-1}(1)L_d - L_d(1)L_{d-1}. \tag{18}$$

Proposition 2.3 implies that $I^\star_{\mathcal{R}_d} L_{d-1} \propto \Pi_{\mathcal{R}^\circ_{d+1}}$, because $I^\star_{\mathcal{R}_d} L_{d-1}$ is orthogonal to $\mathbb{P}_{d-2}$. The definition (15) of $I^\star_{\mathcal{N}}$ and (18) show the relation

$$\Pi_{\mathcal{R}^\circ_{d+1}} \propto I^\star_{\mathcal{R}_d} L_{d-1} = L_{d-1} + \frac{L_d(1)}{L_{d-1}(1)} L_d. \tag{19}$$

For the Lobatto nodes, the polynomial $\Pi_{\mathcal{L}_d}$ can also be guessed, as it must be a linear combination of L_d, L_{d-1} and L_{d-2}. But L_{d-1} does not appear due to opposite parities of $\Pi_{\mathcal{L}_d}$ and L_{d-1} around the midpoint. The condition $\Pi_{\mathcal{L}_d}(0) = 0 = \Pi_{\mathcal{L}_d}(1)$ is ensured if

$$\Pi_{\mathcal{L}_d} \propto L_{d-2}(1)L_d - L_d(1)L_{d-2}. \tag{20}$$

With the definition (15) of $I^\star_{\mathcal{N}}$ we find that $I^\star_{\mathcal{L}_d} L_{d-1} = L_{d-1}$. Taking (20) and Proposition 2.3 into account we obtain

$$\Pi_{\mathcal{L}^\circ_{d+2}} \propto I^\star_{\mathcal{L}_d} L_{d-2} = L_{d-2} + \frac{L_d(1)}{L_{d-2}(1)} L_d. \tag{21}$$

In our numerical experiments, we used the above relations (19) and (21) to set up the test spaces $\mathbb{Q}_{\mathcal{N}}$ as suggested by Proposition 2.3.

The following is a consequence of Lemma 2.2.

Proposition 2.4. *Let $V_h \subset V$ be finite-dimensional. Let $\mathcal{N} \subset [0,1]$ be a set of d distinct nodes. Let $w_h \in \mathbb{P}_d \otimes V_h$. Assume that $f \in \mathbb{P}_d \otimes V'$. Then, with $\mathbb{Q}_{\mathcal{N}}$ as in* (17)*, the collocation condition*

$$((\partial_t + A)w_h(\tau) - f(\tau), \chi_h) = 0 \quad \forall \tau \in \mathcal{N} \quad \forall \chi_h \in V_h$$

is synonymous with the variational statement

$$\int_0^1 ((\partial_t + A)w_h - f, v_h)dt = 0 \quad \forall v_h \in \mathbb{Q}_{\mathcal{N}} \otimes V_h.$$

Proof. The function $p : t \mapsto ((\partial_t + A)w_h(t) - f(t), \chi_h)$ is a polynomial in $\mathbb{P}_d$ for any fixed $\chi_h \in V_h$. The claim therefore follows from Lemma 2.2. □

3. Space-time stability of collocation Runge–Kutta

Given a set of p_n distinct collocation nodes $\mathcal{N}_n$ in the interval $[t_{n-1}, t_n]$ of the n-th step of the Runge–Kutta process (13), we can define $I^\star_{\mathcal{N}_n}$ on $[t_{n-1}, t_n]$ analogously to (15), and $\mathbb{Q}_n := I^\star_{\mathcal{N}_n}\mathbb{P}_{p_n-1}$ analogously to (17). Define $X_h := S^{1,\mathbf{p}}(\mathcal{T}) \otimes V_h$ and $Y_h := V_h \times Y_h^1$ with $Y_h^1 := \{s \in S^{0,\mathbf{p}}(\mathcal{T}) : s|_{(t_{n-1},t_n)} \in \mathbb{Q}_n\} \otimes V_h$. Using Proposition 2.4 transported to each of the intervals $[t_{n-1}, t_n]$ we conclude that the collocation Runge–Kutta process (13) is equivalent to the space-time variational formulation (9)

$$\text{find} \quad u_h \in X_h \quad \text{s.t.} \quad B(u_h, v_h) = F(v_h) \quad \forall v_h \in Y_h, \tag{9}$$

with the present choice of trial X_h and test Y_h spaces, whenever $f \in S^{0,\mathbf{p}}(\mathcal{T}) \otimes V'$ in the definition (8) of the functional F. Let us now address the question of space-time stability (12) of these trial and test spaces.

A crucial ingredient in the proof of the subsequent theorem will be the following lemma. Herein, p' denotes the derivative of p.

Lemma 3.1. *For the Gauß–Legendre nodes one has*

$$(p', I_{\mathcal{G}_d} p)_{L^2(0,1)} = (p', p)_{L^2(0,1)} \quad \forall p \in \mathbb{P}_d, \tag{22}$$

while for the right-Radau nodes,

$$(p', I_{\mathcal{R}_d} p)_{L^2(0,1)} = (p', p)_{L^2(0,1)} + \frac{1}{2}|(p - I_{\mathcal{R}_d} p)(0)|^2 \quad \forall p \in \mathbb{P}_d. \tag{23}$$

Proof. Let $\mathcal{N} \in \{\mathcal{G}_d, \mathcal{R}_d\}$. Take any $p \in \mathbb{P}_d$ and write $p = c\Pi_{\mathcal{N}} + \tilde{p}$ for some $c \in \mathbb{R}$ and some polynomial $\tilde{p} \in \mathbb{P}_{d-1}$. Then $p - I_{\mathcal{N}} p = c\Pi_{\mathcal{N}}$. Observing that $\Pi_{\mathcal{N}}$ is orthogonal to $\mathbb{P}_{d-2}$ in $L^2(0,1)$, one has

$$(p', I_{\mathcal{N}} p - p)_{L^2(0,1)} = -c^2(\Pi'_{\mathcal{N}}, \Pi_{\mathcal{N}})_{L^2(0,1)} = \frac{c^2}{2}\left(|\Pi_{\mathcal{N}}(0)|^2 - |\Pi_{\mathcal{N}}(1)|^2\right).$$

The right-hand-side vanishes in the case of Gauß–Legendre nodes by (anti-)symmetry, hence (22), while $\Pi_{\mathcal{N}}(1) = 0$ in the case of right-Radau nodes yields (23). □

Due to this lemma, in the remainder of this section we shall assume that each $\mathcal{N}_n$ are either the Gauß–Legendre nodes, or the right-Radau nodes, if not stated otherwise.

In connection with this lemma we will further require the following observation: for any polynomial $p \in \mathbb{P}_d$

$$\frac{|(p - I_{\mathcal{N}} p)(0)|^2}{\|p - I_{\mathcal{N}} p\|^2_{L^2(0,1)}} = \frac{|\Pi_{\mathcal{N}}(0)|^2}{\|\Pi_{\mathcal{N}}\|^2_{L^2(0,1)}} = \begin{cases} 2d+1, & \mathcal{N} = \mathcal{G}_d, \\ 4d - 1/d, & \mathcal{N} = \mathcal{R}_d. \end{cases} \tag{24}$$

This can be verified recalling that the orthonormalized Legendre polynomial L_k satisfies $|L_k(0)| = \sqrt{2k+1}$, and using the expression (18) for $\Pi_{\mathcal{R}_d}$.

We define $I : S^{0,\mathbf{p}}(\mathcal{T}) \to S^{0,\mathbf{p}-1}(\mathcal{T})$ and $I^\star : S^{0,\mathbf{p}-1}(\mathcal{T}) \to S^{0,\mathbf{p}}(\mathcal{T})$ element-wise in the obvious way and let $\mathbb{Q} \subset S^{0,\mathbf{p}}(\mathcal{T})$ denote the image of $I^\star$. We write $I^{-\star} := (I^\star)^{-1}$. Let $\mathcal{T}_{\mathcal{R}} := \{t_{n-1} \in \mathcal{T} : \mathcal{N}_n \text{ are right-Radau nodes}\}$ collect the left end-points of the temporal intervals which host right-Radau nodes. Writing Iw, $w \in X_h$, and $I^{-\star}v_1$, $v_1 \in Y_h^1$, etc., the interpolation operator is understood to act on the temporal component, in the same way that Aw sometimes means $(\mathrm{Id} \otimes A)w$. Note that $Y_h = V_h \times I^\star I X_h$, which could also serve as the definition of the discrete test space.

3.1. **Stability in node-dependent norms.** This subsection contains the centerpiece of our analysis, which is Theorem 3.3. In it, we show space-time stability with a constant that is uniform in temporal discretization parameters but in non-uniform space-time norms. Our strategy for further analysis is to relate these discretization parameter dependent norms to the original parabolic space-time norms. This is done in subsequent subsections.

On X_h we define the norm

$$\|w\|_\dagger^2 := \|\partial_t w\|^2_{L^2(J;V')} + \|Iw\|^2_{L^2(J;V)} + \|w(T)\|_H^2 + \sum_{t\in\mathcal{T}_\mathcal{R}} \|(w-Iw)(t^{\leftarrow})\|_H^2, \tag{25}$$

for all $w \in X_h$. The last sum collects contributions of temporal elements that host right-Radau nodes, and $t^{\leftarrow}$ means the limit from the right; the sum is void if Gauß–Legendre nodes are used on each temporal element. The definition is motivated by its role in Theorem 3.3 below, but also by the following observation.

Lemma 3.2. *$\|w(\tau)\|_H \le \|w\|_\dagger$ holds for all $w \in X_h$ and all temporal nodes $\tau \in \mathcal{T}$.*

Proof. Starting with $\|w(\tau)\|_H^2 - \|w(T)\|_H^2 = -2\int_\tau^T (\partial_t w, w)dt$, apply Lemma 3.1 on each temporal element, then the inequalities $|(\partial_t w, Iw)| \le \|\partial_t w\|_{V'}\|Iw\|_V$ and $2ab \le a^2+b^2$. □

Recall symmetry and positivity of A from (5). It is now convenient to introduce an inner product on $Y_h = V_h \times [\mathbb{Q}\otimes V_h]$ by

$$(v,\widetilde{v})_\star := \int_J (I^{-\star}Av_1, I^{-\star}\widetilde{v}_1)dt + (v_0,\widetilde{v}_0), \quad v,\widetilde{v}\in Y_h. \tag{26}$$

Let $\|\cdot\|_\star$ denote the induced norm.

Both, the †- and ⋆-norms, undo the introduction of the adjoint interpolation operator $I^\star$ in the sense that the subsequent theorem could be equivalently formulated for the bilinear form $B_\mathcal{N}$ in (14). An immediate consequence of Lemma 3.2 is that the bilinear forms B in (9) and $B_\mathcal{N}$ in (14) are continuous on $X_h \times Y_h$ equipped with these norms.

As a final preparation for the subsequent theorem set

$$K_h := \inf_{z\in\partial_t X_h\setminus\{0\}} \sup_{v\in Y_h\setminus\{0\}} \frac{\int_J (z,v_1)dt}{\|z\|_{L^2(J;V')}\|v\|_\star}. \tag{27}$$

This quantity is essentially a measure of "self-duality" of V_h, see Section 3.2.1.

Theorem 3.3. *With the definitions and assumptions of this Section,*

$$\inf_{w\in X_h\setminus\{0\}} \sup_{v\in Y_h\setminus\{0\}} \frac{B(w,v)}{\|w\|_\dagger\|v\|_\star} \ge \gamma_{\dagger\star} := \min\{K_h,\alpha,1\}. \tag{28}$$

Proof. Define the linear map $\Gamma : X_h \to Y_h$ by

$$(\Gamma w, v)_\star = B(w,v) \quad \forall (w,v)\in X_h\times Y_h\ . \tag{29}$$

For arbitrary and nonzero $w \in X_h$ we show that $\|\Gamma w\|_\star \ge \gamma_{\dagger\star}\|w\|_\dagger$, which implies the claimed estimate (28) using

$$\sup_{v\in Y_h\setminus\{0\}} \frac{B(w,v)}{\|v\|_\star} = \sup_{v\in Y_h\setminus\{0\}} \frac{(\Gamma w,v)_\star}{\|v\|_\star} = \|\Gamma w\|_\star \ge \gamma_{\dagger\star}\|w\|_\dagger.$$

To that end, we set $v_w := (w(0), I^\star Iw) \in Y_h$, write $\|\Gamma w\|_\star$ as

$$\|\Gamma w\|_\star^2 = \|\Gamma w - v_w\|_\star^2 + 2(\Gamma w, v_w)_\star - \|v_w\|_\star^2, \tag{30}$$

and estimate the individual terms. For the first term in (30), definition (7) of the bilinear form B, definition (26) of the inner product $(\cdot,\cdot)_\star$, and definition (27) of K_h yield

$$\begin{aligned}\|\Gamma w - v_w\|_\star &= \sup_{v\in Y_h\setminus\{0\}} \frac{(\Gamma w - v_w, v)_\star}{\|v\|_\star} \\ &= \sup_{v\in Y_h\setminus\{0\}} \frac{B(w,v) - (v_w,v)_\star}{\|v\|_\star} \\ &= \sup_{v\in Y_h\setminus\{0\}} \frac{\int_J (\partial_t w, v_1)dt}{\|v\|_\star} \geq K_h \|\partial_t w\|_{L^2(J;V')}.\end{aligned}$$

For the second term of (30), we insert v_w in the definition (29) of Γ, apply Lemma 2.1, followed by Lemma 3.1, and evaluate $\int_J(\partial_t w, w)dt$:

$$\begin{aligned}(\Gamma w, v_w)_\star &= \int_J (\partial_t w + Aw, I^\star I w)dt + \|w(0)\|_H^2 \\ &= \int_J (\partial_t w, Iw)dt + \int_J (AIw, Iw)dt + \|w(0)\|_H^2 \\ &= \int_J (\partial_t w, w)dt + \|v_w\|_\star^2 + \frac{1}{2}\sum_{t\in\mathcal{T}_\mathcal{R}} \|(w-Iw)(t^{\leftarrow})\|_H^2 \\ &= \frac{1}{2}\left(\|w(T)\|_H^2 - \|w(0)\|_H^2\right) + \|v_w\|_\star^2 + \frac{1}{2}\sum_{t\in\mathcal{T}_\mathcal{R}} [\text{same}]\,.\end{aligned}$$

Inserting these in (30), combining and estimating further, we obtain $\|\Gamma w\|_\star \geq \gamma_{\dagger\star}\|w\|_\dagger$ as announced. □

We remark that this result remains valid for trial and test spaces with temporally variable spatial discretization constructed as follows. If $V_h^n \subset V$, $n = 0, 1, \ldots, N$, are finite-dimensional subspaces, set the discrete trial space X_h as the collection of all $w \in S^{1,\mathbf{p}}(\mathcal{T}) \otimes V$ satisfying $w(t) \in V_h^{n-1} + V_h^n$ on each temporal element (t_{n-1}, t_n), and $w(t_n) \in V_h^n$ on each temporal node. Take $Y_h := V_h^0 \times I^\star I X_h$ as the definition for the discrete test space. The crucial part is to generalize Lemma 3.1 to vector valued functions of this type, for instance by splitting w into three H-orthogonal parts in V_h^{n-1}, V_h^n and $V_h^{n-1} \cap V_h^n$, on each temporal element.

3.2. **Stability in original norms.** Suppose X_h and Y_h are families of subspaces parameterized by $h > 0$ of the form introduced at the beginning of this section with $\mathcal{T}$ and $\mathbf{p}$ dependent on h. To obtain space-time stability (12) from the estimate (28) of Theorem (3.3), it suffices to verify

a) $K_h \geq K_0 > 0$,
b) $\|\cdot\|_Y \leq C_\star\|\cdot\|_\star$ on Y_h,
c) $\|\cdot\|_X \leq C_\dagger\|\cdot\|_\dagger$ on X_h,

with constants $C_\dagger > 0$, $C_\star > 0$, and $K_0 > 0$ independent of the discretization parameters. Indeed, space-time stability $\inf_{h>0}\gamma_h \geq \gamma_0 > 0$ would follow in (12) with $\gamma_0 := C_\dagger^{-1}C_\star^{-1}\min\{K_0, \alpha, 1\}$. We therefore investigate conditions on the spatial discretization V_h the temporal meshes $\mathcal{T}$, and the polynomial degrees $\mathbf{p}$ (where $\mathcal{T}$ and $\mathbf{p}$ may depend on h) that allow such h-independent constants.

3.2.1. *Approximate self-duality of the spatial discretization.* The quantity K_h defined in (27) only depends on the chosen finite-dimensional subspace $V_h \subset V$, and the operator A. Let us identify $v_1 \neq 0$ in (27) with $\tilde{z} := I^{-\star} v_1 \in Z_h := \partial_t X_h$. Then $\|\tilde{z}\|^2_{L^2(J;V)} \geq \|A\|^{-1} \|(0, v_1)\|^2_\star$. It suffices to take the supremum over $(0, v_1)$ in (27), hence it becomes

$$K_h \geq \|A\|^{-1/2} \inf_{z \in Z_h \setminus \{0\}} \sup_{\tilde{z} \in Z_h \setminus \{0\}} \frac{\int_J (z, \tilde{z}) dt}{\|z\|_{L^2(J;V')} \|\tilde{z}\|_{L^2(J;V)}}.$$

Please note that z and $\tilde{z}$ are measured in different norms. Expanding z and $\tilde{z}$ with respect to an $L^2(J)$ orthonormal basis allows to verify $K_h \geq \|A\|^{-1/2} \kappa_h$, where

$$\kappa_h := \inf_{\chi \in V_h \setminus \{0\}} \sup_{\tilde{\chi} \in V_h \setminus \{0\}} \frac{(\chi, \tilde{\chi})}{\|\chi\|_{V'} \|\tilde{\chi}\|_V} > 0 \tag{31}$$

is a measure of self-duality of V_h. One can show that κ_h^{-1} is the norm of the H-orthogonal projection onto V_h viewed as an endomorphism on V, and therefore κ_h is bounded form below for some commonly used finite element spaces [4, Lemma 6.2].

We show that K_h cannot be removed from (28) in Theorem 3.3, because that would imply a continuity constant $C_h \sim 1$ in (10) when the temporal discretization is sufficiently accurate (that is when the CFL number is small, see below). For simplicity assume additionally that A is an isometry, and that φ_m, $m \in \mathbb{N}$, are H-orthonormal eigenfunctions of A with $A\varphi_m = m^2 \varphi_m$. Then $m^{-1}\varphi_m$ and $m\varphi_m$, $m \in \mathbb{N}$, are orthonormal in V and V', respectively. Define $\chi_M := \sum_{m=1}^M m^{-1} \varphi_m$, and V_h as the span of the single χ_M. Observe that $\zeta_M := \|\chi_M\|^2_H$ and $\|\chi_M\|_{V'} \geq 1$ saturate as $M \to \infty$, while $\|\chi_M\|_V = \sqrt{M}$. Therefore $K_h \geq \kappa_h \sim 1/\sqrt{M}$ for large M. It remains to verify that with this spatial discretization, the stability constant C_h in (10) is not of order one but indeed scales with $\sqrt{M}$. Take $f := 0$ and $g := \chi_M$ in the discrete space-time variational formulation (9) with $X_h := H^1(J) \otimes V_h$ and $Y_h := V_h \times [L^2(J) \otimes V_h]$. It is solved by $t \mapsto u_M(t) = e^{-tM/\zeta_M} \chi_M$, which has $\|u_M\|_X \sim \sqrt{M}$ for large M. But $\|F\|_{Y'} \sim 1$, hence $C_h \sim \sqrt{M}$ in (10) for large M, as claimed.

3.2.2. *Norm comparison on the test space.* In this subsection we address the norm comparison $\|\cdot\|_Y \leq C_\star \|\cdot\|_\star$ on Y_h. We estimate as follows,

$$\begin{aligned}
\|v\|^2_Y &= \|I^\star I^{-\star} v_1\|^2_{L^2(J;V)} + \|v_0\|^2_H \\
&\leq \|I^\star\|^2 \|I^{-\star} v_1\|^2_{L^2(J;V)} + \|v_0\|^2_H \\
&\leq \max\{\|I^\star\|^2/\alpha^2, 1\} \left(\alpha^2 \|I^{-\star} v_1\|^2_{L^2(J;V)} + \|v_0\|^2_H \right) \leq C^2_\star \|v\|^2_\star
\end{aligned}$$

for any $v = (v_0, v_1) \in Y_h$ with the constant $C_\star := \max\{\|I^\star\|/\alpha, 1\}$, using positivity (5) of A. Thus it remains to estimate $\|I^\star\|$.

As noted following (15), the operator norm of $(I^\star_{\mathcal{N}})^{-1}$, induced by the $L^2(0,1)$ norm, is bounded by one irrespectively of the choice of d distinct nodes $\mathcal{N} \subset [0,1]$. Let us comment on the norm of $I^\star_{\mathcal{N}}$, which, in view of (16), is the same as that of $I_{\mathcal{N}}$, and is invariant under rescaling of the interval.

a) If $\mathcal{N} \subset (0,1)$ are the Gauß–Legendre nodes then $I^\star_{\mathcal{N}}$ is the identity, hence of unit norm.

b) Let $\mathcal{N} \subset (0,1]$ be the d right-Radau nodes for the interval $[0,1]$. Since $\Pi_{\mathcal{R}_d}$ is a multiple of $L_d(1)L_{d-1} - L_{d-1}(1)L_d$, see (18), one can compute

$$\|I^\star_{\mathcal{N}}\|^2 = \|I^\star_{\mathcal{N}} L_{d-1}\|^2_{L^2(0,1)} = 1 + \left|\frac{L_d(1)}{L_{d-1}(1)}\right|^2 = 1 + \frac{2d+1}{2d-1}.$$

Thus, $\|I^\star_{\mathcal{N}}\| \le 2$ for Radau nodes $\mathcal{N}$ of any order.

c) Similarly, $\|I^\star_{\mathcal{L}_d}\|^2 = 1 + (2d+1)/(2d-3) \le 6$ holds for the Lobatto nodes.

d) For general d nodes one can show $\|I_{\mathcal{N}}\| = \|I^\star_{\mathcal{N}}\| \le 1 + (2d)!/(d!)^2 \le 1 + 4^d$.

Now recall that we have assumed the test space Y_h to be based on Gauß–Legendre or right-Radau nodes. Then $\|I^\star_{\mathcal{N}}\| \le 2$ as discussed above, and we obtain the desired norm comparison uniformly in the discretization parameters, in particular in the polynomial degrees. More precisely, $\|I^\star\| \le 1$ if only Gauß–Legendre nodes are used, and $\|I^\star\| \le 2$ if also right-Radau nodes are admitted. These are responsible for the asymptotic behavior of the space-time stability constant observed in Figure 1.3.

3.2.3. *Norm comparison on the trial space.* In this subsection we obtain the norm comparison $\|\cdot\|_X \le C_\dagger \|\cdot\|_\dagger$ on X_h. The constant $C_\dagger$, however, depends on the discretization parameters, and the goal of this subsection is to investigate this dependence. To that end we introduce the CFL number. We abbreviate

$$\Lambda_h := \sup_{\chi \in V_h \setminus \{0\}} \frac{\|\chi\|_V}{\|\chi\|_H} \tag{32}$$

and on each temporal element we define the local CFL number

$$\mathrm{CFL}_n := |t_n - t_{n-1}|\, \Lambda_h^2, \quad n = 1, \dots, N. \tag{33}$$

One can see from the parabolic evolution equation (4) that the CFL number is dimension-free. Moreover, Λ_h is the same if the pair (V,H) is replaced by (H,V') in (32). The (global) CFL number is the maximum of all local ones, $\mathrm{CFL} := \max_{n=1,\dots,N} \mathrm{CFL}_n$. We remark that below the local CFL number always appears in conjunction with the local polynomial degree, but we chose not to include these in the definition (33).

For convenience, we recall here the two norms $\|\cdot\|_X$ and $\|\cdot\|_\dagger$ defined for all $w \in X_h$ as

$$\|w\|_X^2 := \|\partial_t w\|^2_{L^2(J;V')} + \|w\|^2_{L^2(J;V)} + \|w(T)\|_H^2, \tag{2}$$

$$\|w\|_\dagger^2 := \|\partial_t w\|^2_{L^2(J;V')} + \|Iw\|^2_{L^2(J;V)} + \|w(T)\|_H^2 + \sum_{t \in \mathcal{T}_{\mathcal{R}}} \|(w - Iw)(t^{\leftarrow})\|_H^2, \tag{25}$$

where $\mathcal{T}_{\mathcal{R}}$ are the left endpoints of the temporal elements with right-Radau nodes, and $t^{\leftarrow}$ means the limit from the right.

To obtain the desired norm comparison $\|\cdot\|_X \le C_\dagger \|\cdot\|_\dagger$, we need to estimate $\|w\|_{L^2(J;V)}$ in terms of $\|w\|_\dagger$, or if more convenient $\|w - Iw\|_{L^2(J;V)}$ in terms of the same, since for all $\epsilon > 0$ there holds

$$\|w\|^2_{L^2(J;V)} \le (1 + \epsilon^{-2}) \|Iw\|^2_{L^2(J;V)} + (1 + \epsilon^2) \|w - Iw\|^2_{L^2(J;V)}. \tag{34}$$

If only Gauß–Legendre nodes are present, the sharper orthogonality relation

$$\|w\|^2_{L^2(J;V)} = \|Iw\|^2_{L^2(J;V)} + \|w - Iw\|^2_{L^2(J;V)} \tag{35}$$

is at our disposal.

We look at estimates that are valid on each interval. These correspond to the three types of behavior observed in Figure 1.3 in the introduction.

a) For the temporal elements that host right-Radau nodes, the sum in the $\|\cdot\|_\dagger$-norm, see (25), is useful for the norm comparison. Let $J_n := (t_{n-1}, t_n)$ be such a temporal element with p_n right-Radau nodes $\mathcal{N}_n \subset (t_{n-1}, t_n]$. On J_n we have $w - Iw = \Pi_{\mathcal{N}_n} \otimes \chi_n$ with some $\chi_n \in V_h$, and therefore

$$\|w - Iw\|_{L^2(J_n;V)} = \frac{\|\Pi_{\mathcal{N}_n}\|_{L^2(J_n)}}{|\Pi_{\mathcal{N}_n}(t_{n-1})|} \|(w - Iw)(t_{n-1}^{\leftarrow})\|_V. \tag{36}$$

Using (24) for $\Pi_{\mathcal{N}_n}$ and the definition of the local CFL number (33) we find (note the squares)

$$\|w - Iw\|^2_{L^2(J_n;V)} \leq \frac{\mathrm{CFL}_n}{4p_n - 1/p_n} \|(w - Iw)(t_{n-1}^{\leftarrow})\|^2_H. \tag{37}$$

If only right-Radau nodes are present we obtain the norm comparison $\|\cdot\|_X \leq C_\dagger \|\cdot\|_\dagger$ from (34) with a constant

$$C_\dagger^2 \leq \inf_{\epsilon>0} \max\{1 + \epsilon^{-2}, (1+\epsilon^2)\,\mathrm{CFL}\,/3\} = 1 + \mathrm{CFL}\,/3. \tag{38}$$

This explains the preasymptotic behavior of the stability constant (10) for the backward Euler time-stepping scheme in Figure 1.3. A competing estimate for right-Radau nodes is derived in Section 3.4 below.

b) On the temporal intervals that host Gauß–Legendre nodes we have no control on point values explicitly in the norm $\|\cdot\|_\dagger$, but Lemma 3.2 gives a hint. Consider a set of Gauß–Legendre nodes $\mathcal{N} = \mathcal{G}_d$ of arbitrary order on the unit interval $(0,1)$. Then from (24) we have, followed by a similar procedure as in (34),

$$\begin{aligned}(2d+1)\|p - I_{\mathcal{N}} p\|^2_{L^2(0,1)} &= |(p - I_{\mathcal{N}} p)(0)|^2 \\ &\leq (1+\epsilon^{-2})|I_{\mathcal{N}} p(0)|^2 + (1+\epsilon^2)|p(0)|^2 \\ &\leq (1+\epsilon^{-2}) d^2 \|I_{\mathcal{N}} p\|^2_{L^2(0,1)} + (1+\epsilon^2)|p(0)|^2.\end{aligned}$$

The last inequality is seen by expanding $I_{\mathcal{N}} p$ into the Legendre polynomials, evaluating at zero, estimating with Cauchy–Schwartz, and computing $\sum_{k=0}^{d-1}(2k+1) = d^2$. For a set of p_n Gauß–Legendre nodes $\mathcal{N}_n$ on $J_n = (t_{n-1}, t_n)$ and any vector-valued polynomial $w \in \mathbb{P}_{p_n} \otimes V_h$ we obtain

$$\begin{aligned}&\|w - Iw\|^2_{L^2(J_n;V)} \leq \\ &\leq (1+\epsilon^{-2}) \frac{p_n^2}{2p_n+1} \|Iw\|^2_{L^2(J_n;V)} + (1+\epsilon^2) \frac{|t_n - t_{n-1}|}{2p_n+1} \|w(t_{n-1})\|^2_V &\text{(39a)}\\ &\leq (1+\epsilon^{-2}) \frac{p_n}{2} \|Iw\|^2_{L^2(J_n;V)} + (1+\epsilon^2) \frac{\mathrm{CFL}_n}{3} \|w\|^2_\dagger, &\text{(39b)}\end{aligned}$$

where in the second inequality we used $\|w(\tau)\|_H \leq \|w\|_\dagger$ from Lemma 3.2 and the definition (33) of the local CFL number.

Note that $\sum_{n=1}^N \mathrm{CFL}_n = T\Lambda_h^2$. Thus, if only Gauß–Legendre node are present, we sum up over all temporal elements and use (35) to find the norm comparison

$\|w\|_X \le C_\dagger \|w\|_\dagger$ with

$$C_\dagger^2 \le \inf_{\epsilon>0} \left\{ 1 + \frac{1+\epsilon^{-2}}{2} |\mathbf{p}|_\infty + \frac{1+\epsilon^2}{3} T\Lambda_h^2 \right\}, \tag{40}$$

where we have taken the same ϵ for each temporal element and estimated p_n by the maximal occuring polynomial degree $|\mathbf{p}|_\infty$. This explains the initial stagnation of the stability constant (10) for the implicit midpoint rule time-stepping scheme in Figure 1.3. In the case of a single temporal element, $T\Lambda_h^2 = \mathrm{CFL}$, and the bounds in (38) and (40) are very close. This is confirmed by Figure 1.3.

c) When the CFL number is small, another type of inverse inequality becomes relevant. Again, we first consider the reference unit interval. Let $\mathcal{N} \subset [0,1]$ be a set of distinct collocation nodes. Take any polynomial $p \in \mathbb{P}_d$ of degree $d \ge 1$. Then $p = \Pi_\mathcal{N} + I_\mathcal{N} p$, where the coefficient of the leading monomial was assumed to be one without loss of generality. Its derivative is $p' = \Pi'_\mathcal{N} + (I_\mathcal{N} p)'$. The polynomial $(I_\mathcal{N} p)'$, if nonzero, is of lower degree than $\Pi'_\mathcal{N}$, which implies $\|p'\|_{L^2(0,1)} \ge |(\Pi'_\mathcal{N}, L_{d-1})_{L^2(0,1)}|$. We arrive at

$$\|p - I_\mathcal{N} p\|_{L^2(0,1)} \le C'_\mathcal{N} \|p'\|_{L^2(0,1)}, \quad C'_\mathcal{N} := \frac{\|\Pi_\mathcal{N}\|_{L^2(0,1)}}{|(\Pi'_\mathcal{N}, L_{d-1})_{L^2(0,1)}|}.$$

For Gauß–Legendre and right-Radau nodes the denominator equals $|\Pi_\mathcal{N}(1) L_{d-1}(1) - \Pi_\mathcal{N}(0) L_{d-1}(0)|$, as can be seen after integration by parts. With this, and the expression (18) for $\Pi_{\mathcal{R}_d}$,

$$C'_{\mathcal{G}_d} = \frac{1}{2\sqrt{4d^2-1}} \quad \text{and} \quad C'_{\mathcal{R}_d} = \frac{2}{\sqrt{2-1/d}} C'_{\mathcal{G}_d} \le 2C'_{\mathcal{G}_d}.$$

The bound $C'_{\mathcal{R}_d} \le 2C'_{\mathcal{G}_d} \le 1/\sqrt{3}$ is again uniform in the polynomial degree d. For a set of p_n Gauß–Legendre or right-Radau nodes $\mathcal{N}_n$ on the temporal element $J_n = (t_{n-1}, t_n)$ and any vector-valued polynomial $w \in \mathbb{P}_{p_n} \otimes V_h$ we obtain

$$\|w - Iw\|_{L^2(J_n;V)} \le C'_{\mathcal{N}_n} \,\mathrm{CFL}_n \, \|\partial_t w\|_{L^2(J_n;V')}, \tag{41}$$

where $C'_{\mathcal{N}_n}$ is either $C'_{\mathcal{G}_d}$ or $C'_{\mathcal{R}_d}$ with $d = p_n$. Therefore $\mathrm{CFL} \lesssim 1$ entails $C_\dagger \sim 1$ in the norm comparison $\|\cdot\|_X \le C_\dagger \|\cdot\|_\dagger$.

When only Gauß–Legendre nodes are present, orthogonality of Iw and $(w - Iw)$ (35) allows to choose $C_\dagger^2 \le 1 + \mathrm{CFL}^2/12$. Thus the behavior of the implicit midpoint rule time-stepping scheme in Figure 1.3 is explained also in the regime of moderate CFL numbers.

In summary we have found for Gauß–Legendre and right-Radau nodes the norm comparison of the form

$$\|\cdot\|_X \le C_\dagger \|\cdot\|_\dagger \quad \text{with} \quad C_\dagger := C \min\{|\mathbf{p}|_\infty + \sqrt{T}\Lambda_h, 1 + \mathrm{CFL}\}$$

and if only right-Radau nodes are present the improved estimate

$$\|\cdot\|_X \le C_\dagger \|\cdot\|_\dagger \quad \text{with} \quad C_\dagger := 1 + C\sqrt{\mathrm{CFL}}.$$

The constant $C > 0$ can be chosen independently of all parameters, in particular nonincreasing with the polynomial degrees.

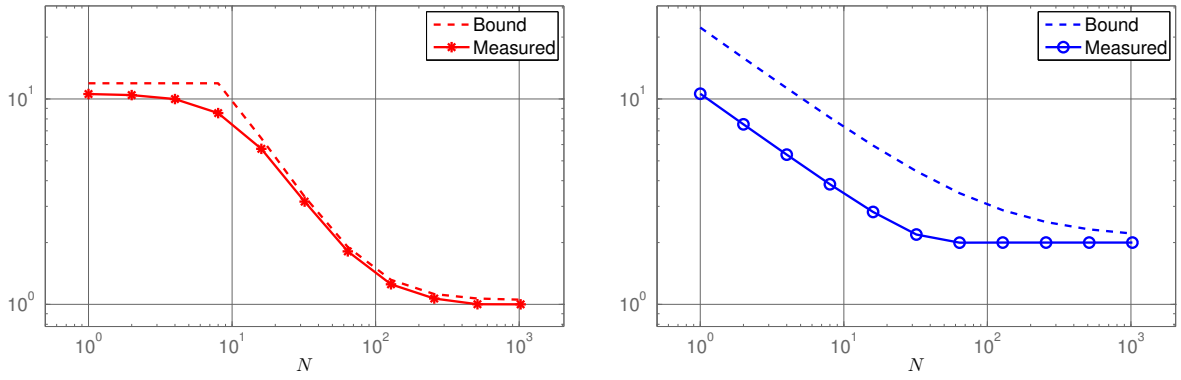

FIGURE 2. Space-time stability constant for implicit midpoint rule (**left**) and backward Euler (**right**) time-stepping schemes as a function of the number N of equidistant time-steps, see Section 1.3, together with the analytical bounds discussed in Section 3.2.

3.2.4. *Numerical evaluation of the bounds.* We return to the example discussed in Section 1.3 and compare the measured stability constant C_h in (10) with the bounds derived in this Section. The bound $C_h \le \gamma_0^{-1}\|B\|$ is composed as follows: $\|B\| \le 1$, see Subsection 1.2, and $\gamma_0 := C_\dagger^{-1} C_\star^{-1} \min\{K_h, \alpha, 1\}$, where $\alpha = 1$ in this example, and we replace $C_\star$ by the estimate derived in Subsection 3.2.2 and $C_\dagger$ by the estimates derived in Subsection 3.2.3. We computed $K_h \approx 0.9528$ and $\Lambda_h \approx 4.0942$. Figure 3.2.4 shows validity of the estimates and good agreement with the measured stability constant.

We remark that our bounds on the various quantities may be not active simultaneously, which leads to overestimation of the stability constant C_h in certain cases. For instance, for the backward Euler time-stepping scheme, see Figure 3.2.4 (right), the bound on $C_\dagger$ and the bound on $\|I^\star\|$ together yield an overestimate by a factor ≈ 2 when the CFL number is large. Indeed, we observe numerically that in the case of a single temporal element the optimizing pair $(w, v) \in X_h \times Y_h$ in the discrete inf-sup constant (28) may have the property that $\|I^{-\star} v_1\|_{L^2(J;V)}$ is much smaller than $\|v_0\|_H$, and therefore estimating $\|v\|_Y \le \|I^\star\| \|v\|_\star$ as we did in Subsection 3.2.2 is too pessimistic by a factor of approximately $\|I^\star\| = 2$.

3.3. **Analysis of the Lobatto nodes.** Recall that Lemma 3.1 on Gauß–Legendre and right-Radau nodes entered the proof of Theorem 3.3 and was crucial for the aforegoing analysis. As a substitute for Lemma 3.1 for the $d+1$ Lobatto nodes, $d \in \mathbb{N}$, we shall exploit the relation

$$(p', q)_{L^2(0,1)} = ((I_{\mathcal{L}_{d+1}} p)', q)_{L^2(0,1)} \quad \forall (p, q) \in \mathbb{P}_{d+1} \times \mathbb{P}_{d-1}. \tag{42}$$

Integration by parts shows that this is equivalent to $(p - I_{\mathcal{L}_{d+1}} p, q')_{L^2(0,1)} = 0$ for the same p and q. This in turn is true because the integrand is a polynomial of degree $2d-1$ vanishing on the Lobatto nodes $\mathcal{L}_{d+1}$, which are exact on $\mathbb{P}_{2d-1}$.

Let the discrete trial space $X_h := S^{1,\mathbf{p}}(\mathcal{T}) \otimes V_h$ be the space of the same form as in the beginning of this Section, and let the discrete test space Y_h be based on Gauß–Legendre nodes. We increase the polynomial degrees by one to obtain $\widehat{X}_h := S^{1,\mathbf{p}+1}(\mathcal{T}) \otimes V_h$, and let $\widehat{Y}_h = V_h \times \widehat{Y}_h^1$ denote the corresponding discrete test space that is based on Lobatto nodes. The compound interpolation operators are denoted accordingly by I and $\widehat{I}$. Assume that $f \in S^{0,\mathbf{p}}(\mathcal{T}) \otimes V'$ and $g \in H$. Let u_h (and $\widehat{u}_h$) denote the solution to the discrete space-time

variational formulation (9) with $X_h \times Y_h$ (replaced by $\widehat{X}_h \times \widehat{Y}_h$). We now estimate $\|\widehat{u}_h\|_X$ from above in terms of $\|u_h\|_X$.

Let us write $U_h := \widehat{I}\widehat{u}_h$ for discrete solution based on the Lobatto nodes interpolated on the same. From the identity of the stability functions $R_{\mathcal{L}_{d+1}} = R_{\mathcal{G}_d}$ stated in Subsection 2.2 it is clear that U_h and u_h coincide on the mesh nodes $\tau \in \mathcal{T}$, in particular $U_h(0) = u_h(0)$. We claim that in fact $U_h = u_h$. To prove this we verify that $U_h \in X_h$ satisfies the discrete space-time variational formulation (9) that caracterizes u_h. Therefore we use the aforegoing relation (42), exactness of $\widehat{I}$ on $S^{0,\mathbf{p}}(\mathcal{T})$, and $\widehat{I}^\star v_1 \in \widehat{Y}_h^1$ for any $v_1 \in Y_h^1$, to compute

$$\begin{aligned}\int_J (\partial_t U_h + AU_h - f, v_1)dt &= \int_J (\widehat{I}(\partial_t \widehat{u}_h + A\widehat{u}_h - f), v_1)dt \\ &= \int_J (\partial_t \widehat{u}_h + A\widehat{u}_h - f, \widehat{I}^\star v_1)dt = 0.\end{aligned}$$

As noted, the initial values coincide, $U_h(0) = u_h(0)$, and thus $U_h = u_h$.

These ingredients allow to estimate

$$\|\widehat{u}_h\|_X^2 \leq \|\partial_t \widehat{u}_h\|^2_{L^2(J;V')} + 2\|\widehat{u}_h - \widehat{I}\widehat{u}_h\|^2_{L^2(J;V)} + 2\|u_h\|^2_{L^2(J;V)} + \|u_h(T)\|_H^2.$$

We employ the inverse estimate $\|\widehat{u}_h - \widehat{I}\widehat{u}_h\| \leq \mathrm{CFL}/\sqrt{10}\|\partial_t \widehat{u}_h\|$ as in (41) for the second term on the right, and collect with the first term. Inserting $\partial_t \widehat{u}_h = -Au_h + \widehat{I}f$ and estimating further we arrive at $\|\widehat{u}_h\|_X \leq \widehat{C}_h \|F\|_{Y'}$, with $\widehat{C}_h \leq 2(1 + 2\,\mathrm{CFL}^2/10)((\|A\|^2 + 1)C_h^2 + 1)$ where C_h is the stability constant for u_h from (10). Thus, as for C_h, we expect a three-phase behavior for $\widehat{C}_h$: as the number of temporal intervals increases, it is proportional to the CFL number, then the square of the CFL number, and is eventually of order one. The estimate is pessimistic roughly by a factor of four for large CFL numbers. We indeed observe this in our numerical experiments for the two point Lobatto collocation in the set-up of Section 1.3, see Figure 3.4, where also the derived bound is shown.

3.4. **Temporal mesh with geometric warm up.** Using the relation (36) and continuity of the discrete solution w, one can estimate the defect $w - Iw$ on the temporal element $J_{n+1} = (t_n, t_{n+1})$ in terms of the quantities available in $\|w\|_\dagger$ if the preceding temporal element $J_n = (t_{n-1}, t_n)$ hosts right-Radau nodes. In this situation, observe that $Iw(^\rightarrow t_n) = w(^\rightarrow t_n) = w(t_n^\leftarrow)$, because t_n is a collocation point in $\mathcal{N}_{p_n}$ on the temporal element J_n, where $^\rightarrow t_n$ denotes the limit from the left. Thus we can estimate $\|(w - Iw)(t_n^\leftarrow)\|_V \leq \|Iw(^\rightarrow t_n)\|_V + \|Iw(t_n^\leftarrow)\|_V$ in (36). For the sake of clarity, let us again assume that all temporal intervals host right-Radau nodes. We write $|J_n|$ for the length of the temporal element J_n. Similarly to (37) and (39) we find

$$\|w - Iw\|^2_{L^2(J_{n+1};V)} = \frac{|J_{n+1}|}{4p_{n+1} - 1/p_{n+1}} \|(w - Iw)(t_n^\leftarrow)\|_V^2 \tag{43a}$$

$$\leq \frac{|J_{n+1}|}{3} \left[\frac{p_n}{\sqrt{|J_n|}} \|Iw\|_{L^2(J_n;V)} + \frac{p_{n+1}}{\sqrt{|J_{n+1}|}} \|Iw\|_{L^2(J_{n+1};V)} \right]^2 \tag{43b}$$

$$\leq \frac{2}{3}|\mathbf{p}|_\infty^2 \left(\frac{|J_{n+1}|}{|J_n|} \|Iw\|^2_{L^2(J_n;V)} + \|Iw\|^2_{L^2(J_{n+1};V)} \right). \tag{43c}$$

Set $\sigma := \max_{1,\dots,N-1} |J_{n+1}|/|J_n|$ for the maximal ratio of the lengths of neighboring temporal elements. Collecting all defects and using (37) on the first temporal element, we obtain the

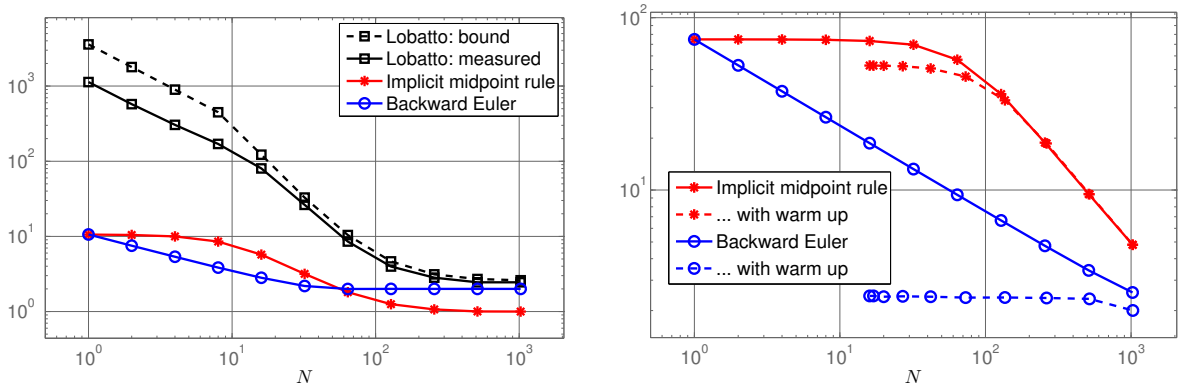

FIGURE 3. Space-time stability constant for implicit midpoint rule and backward Euler time-stepping schemes as a function of the number N of temporal elements. **Left**: Comparison with the two point Lobatto collocation Runge–Kutta, see Section 3.3. **Right**: The effect of the "geometric warm up", see Section 3.4.

norm comparison $\|\cdot\|_X \le C_\dagger \|\cdot\|_\dagger$ with

$$C_\dagger^2 \le \inf_{\epsilon>0} \max\left\{\frac{1}{3}(1+\epsilon^2)\,\mathrm{CFL}_1, (1+\epsilon^{-2}) + \frac{2}{3}(1+\epsilon^2)|\mathbf{p}|_\infty^2(\sigma+1)\right\}.$$

Note that only the local CFL number of the first temporal element enters the estimate. This suggests a "geometric warm up" strategy for positioning the temporal nodes in order to improve the space-time stability constant. To illustrate this we revisit the example from Section 1.3. For each uniform temporal mesh we subdivide the first temporal element J_1 using geometric refinement towards the origin by appending the nodes $\sigma^{-\ell}|J_1|$, $\ell = 1, 2, \ldots$, for which $\sigma^{-\ell}|J_1|\Lambda_h^2 \ge 1$, where $\sigma := 2$. To render the stabilizing effect more visible we set $T = 1000$ for the end time. The results, see Figure 3.4, show that for the backward Euler time-stepping scheme (unlike for the implicit midpoint rule) the "geometric warm up" strategy renders the space-time stability constant of order one, uniformly in the initial number of temporal elements, at the expence of only a few more.

The local CFL number of the first temporal element appears in the above estimate because we assumed $g \in H$ for the initial datum in (8) but can be dropped if g is more regular, say $g \in V$. From the discrete space-time variational formulation (9) it is clear that $w(0)$ is the H-orthogonal projection of g onto V_h. From Section 3.2.1 we have $\|w(0)\|_V \le \kappa_h^{-1}\|g\|_V$, where κ_h is the measure of self-duality (31) of V_h. With this in mind let us revisit the estimate (43) on the first temporal element:

$$\|w - Iw\|_{L^2(J_1;V)}^2 \le \frac{2}{3}|J_1|\kappa_h^{-2}\|g\|_V^2 + \frac{2}{3}p_1^2\|Iw\|_{L^2(J_1;V)}^2.$$

As noted in Section 3.2.1, one can bound κ_h from below for some common finite element spaces V_h, thus we may assume that $|J_1|\kappa_h^{-2}\|g\|_V^2$ is bounded above by a certain g-dependent constant multiple of $\|F\|_{Y'}^2$. Using this estimate instead of (37) on the first temporal element leads to a space-time stability constant C_h in (10) that only depends on the operator A, the initial datum g, the lower bound on κ_h, the end time T, the polynomial degrees $\mathbf{p}$ and the interelement ratio σ (or upper bounds on T, $\mathbf{p}$ and σ), but not the CFL number.

4. Conclusions

We have shown that collocation Runge–Kutta time-stepping schemes applied to a spatially semi-discretized linear parabolic evolution equation produce a solution that a priori depends continuously on the input data in a parabolic space-time norm, but the continuity constant may be large, unless the parabolic CFL number is of order one. If one is interested in a moderate continuity constant, for instance for space-time simultaneous solution and preconditioning of the parabolic evolution equation, or residual based a posteriori error estimation, this entails restrictions on the time step size even if these schemes are A- or L-stable.

To arrive at this conclusion, we have formulated collocation Runge–Kutta time-stepping schemes as Petrov–Galerkin methods for a space-time variational formulation of an abstract linear parabolic evolution equation. The main ingredient in the construction of the appropriate discrete test spaces is the adjoint of the interpolation operator. For collocation Runge–Kutta time-stepping schemes based on Gauß–Legendre, right-Radau and Lobatto nodes, we have analyzed the a priori stability of the resulting Petrov–Galerkin method, and we have shown that the stability constant is linked to the parabolic CFL number. We stress that this a priori analysis does not assume any additional smoothness of the exact solution, the initial datum, or the residual; we plan to comment on the implications of smoothness and the relation to the classical convergence analysis elsewhere.

Our numerical experiments for the heat equation indicate that the bounds are, up to a small constant, sharp. In fact, it is possible to construct examples which verify that the scaling of the stability constant with respect to the CFL number cannot be improved in general. These are highly oscillatory in time functions in the case of Gauß–Legendre nodes such that Iw is small in (39), and functions supported on the first temporal element in the case of right-Radau nodes for which (37) is the only available estimate. On the other hand, in the case of right-Radau nodes the restriction on the time step size can be circumvented by applying a "geometric warm up" strategy on the first temporal element tailored to the spatial discretization, or by assuming a sufficiently regular initial datum.

Acknowledgement

RA acknowledges the hospitality of the Seminar for Applied Mathematics, ETH Zürich, where this work was initiated.

References

[1] Georgios Akrivis, Charalambos Makridakis, and Ricardo Nochetto. Galerkin and Runge-Kutta methods: unified formulation, a posteriori error estimates and nodal superconvergence. *Numer. Math.*, 118:429–456, 2011. 1.2, 2.1

[2] Jochen Alberty, Carsten Carstensen, and Stefan A. Funken. Remarks around 50 lines of Matlab: short finite element implementation. *Numer. Algorithms*, 20(2-3):117–137, 1999. 1.3

[3] Roman Andreev. Space-time discretization of the heat equation. A concise Matlab implementation. *ArXiv e-prints*, December 2012. 1.3

[4] Roman Andreev. Stability of sparse space-time finite element discretizations of linear parabolic evolution equations. *IMA J. Numer. Anal.*, 33(1):242–260, 2013. 3.2.1

[5] Ivo Babuška and Tadeusz Janik. The h-p Version of the Finite Element Method for Parabolic Equations. II. The h-p Version in Time. *Numerical Methods for Partial Differential Equations*, 6:343–369, 1990. 1.2

[6] Walter Gautschi. *Orthogonal polynomials. Computation and Approximation.* Numerical Mathematics and Scientific Computation. Oxford University Press Inc., 2004. 2.2, 2.3, 2.3

[7] Ernst Hairer and Gerhard Wanner. *Solving ordinary differential equations. II*, volume 14 of *Springer Series in Computational Mathematics*. Springer-Verlag, Berlin, 2010. Second revised edition. 2.2

[8] Bernie L. Hulme. Discrete Galerkin and related one-step methods for ordinary differential equations. *Math. Comp.*, 26:881–891, 1972. 1.2
[9] Jacques-Louis Lions and Enrico Magenes. *Non-homogeneous boundary value problems and applications. Vol. I.* Springer-Verlag, New York, 1972. Translated from the French by P. Kenneth, Die Grundlehren der mathematischen Wissenschaften, Band 181. 1.1, 1.1
[10] Charalambos Makridakis and Ivo Babuška. On the stability of the discontinuous Galerkin method for the heat equation. *SIAM J. Numer. Anal.*, 34(1):389–401, 1997. 1.2
[11] Jinchao Xu and Ludmil Zikatanov. Some observations on Babuška and Brezzi theories. *Numer. Math.*, 94(1):195–202, 2003. 1.2

(Roman Andreev) Radon Institute for Computational and Applied Mathematics, Austrian Academy of Sciences, Altenbergerstr. 69, 4040 Linz, Austria
E-mail address: roman.andreev@oeaw.ac.at

(Julia Schweitzer) Institute for Applied and Numerical Mathematics 1, Karlsruhe Institute of Technology, Kaiserstr. 89-93, D-76133 Karlsruhe, Germany
E-mail address: julia.schweitzer@kit.edu